
Supplementary information

**Three-dimensional folding dynamics of the
Xenopus tropicalis genome**

In the format provided by the
authors and unedited

1 (Supplementary information contains 19 figures, 5 tables, and 3 sourcedata
2 files.)

3

4 **Supplementary Fig. 1 | Heatmap of each chromosome.** Assembly errors are
5 mostly corrected in both Niu et al. and v10.0 versions of the reference genome.
6 Arrows point to obvious errors in both Niu et al. and v10.0 versions.

7

8 **Supplementary Fig. 2 | Genome-wide contact heatmap.** Centromere
9 interactions are weak using the v9.1 *X. tropicalis* reference genome.
10 Genome-wide contact heatmaps show intra-chromosome arm interactions and
11 inter-chromosome interactions between centromeres using Niu et al. and
12 v10.0 versions of the reference genome.

13

14 **Supplementary Fig. 3 | Convergent CTCF site distribution and western blot.**
15 **a,** Accumulated convergent CTCF sites observed at all borders of TADs (in ten
16 thousands) identified at all developmental stages.
17 **b,** Western blot of CTCF and Rad21 at different developmental stages.
18 Western blot experiments in this figure were repeated for at least two times
19 with similar results.

20

21 **Supplementary Fig. 4 | CTCF ChIP-seq on wild type embryos.**

22 **a,** CTCF ChIP-seq on embryos from stages 8, 9, 11, and 13 normalized to

23 CTCF ChIP-seq signal from spike-in K562 cells.

24 **b**, CTCF ChIP-seq on spike-in K562 cells.

25

26 **Supplementary Fig. 5** | Rad21 ChIP-seq on wild type embryos

27 **a**, Rad21 ChIP-seq on embryos from stages 9, 11 and 13 normalized to Rad21

28 ChIP-seq signal from spike-in K562 cells.

29 **b**, Rad21 ChIP-seq on spike-in K562 cells.

30

31 **Supplementary Fig. 6** | Examples of TADs for the three different clusters.

32 **a**, **b**, and **c**, Example TADs in clusters 1, 2, and 3. Paired TADs in hierarchical

33 TAD can also be seen in **c**. Red, black, and blue triangles indicate TADs in

34 clusters 1, 2, and 3, respectively.

35

36 **Supplementary Fig. 7** | Directionality index analysis in human K562 cells.

37 **a**, Directionality index across borders of the three clusters of TADs in K562

38 cells. Cluster 2 shown in the DI heatmap is further divided into five sub-clusters

39 with the same number of TADs.

40 **b**, Enrichment of CTCF is biased to borders with higher directionality index

41 values for the three clusters of TADs. CTCF enrichment is shown in the

42 heatmap.

43 **c**, Enrichment of Rad21 is biased to borders with higher directionality index

44 values for the three clusters of TADs. Rad21 enrichment is shown in the

45 heatmap. Data in upper panels of **a**, **b**, and **c** are represented as mean \pm SEM.
46 **d**, Directionality bias index for the five sub-clusters of cluster 2. According to
47 the rank of directionality index strength, TADs in cluster 2 are divided into five
48 sub-clusters. Data are presented as boxplots with violinplots. The minima,
49 maxima, center, and bounds of each boxplot refers to Q1-1.5IQR, Q3+1.5IQR,
50 median, first quartile (Q1) and third quartile (Q3) of data. IQR, interquartile
51 range.
52 **e**, Enrichment of CTCF is slightly biased to borders with a higher directionality
53 index for the five sub-clusters of cluster 2. According to the rank of
54 directionality index strength, TADs in cluster 2 are divided into five
55 sub-clusters.
56 **f**, Enrichment of Rad21 is slightly biased at borders with a higher directionality
57 index for the five clusters 2 sub-clusters. According to the rank of directionality
58 index strength, TADs in cluster 2 are divided into five sub-clusters. Data in **e**
59 and **f** are represented as mean \pm SEM.

60

61 **Supplementary Fig. 8|Directionality index analysis in *Drosophila* S2 cells.**

62 **a**, Directionality index across borders of clustered TADs of *Drosophila* S2 cells.

63 150, 466, and 182 TADs in Clusters 1, 2, and 3, respectively. C, cluster.

64 **b**, Violin plot showing the distribution of directionality bias index of clusters 1, 3,

65 and five sub-clusters of cluster 2 in *Drosophila* S2 cells. Data are presented as

66 boxplots with violinplots. The minima, maxima, center, and bounds of each

67 boxplot refers to Q1-1.5IQR, Q3+1.5IQR, median, first quartile (Q1) and third
68 quartile (Q3) of data. IQR, interquartile range.

69 **c**, Relative enrichment of CTCF at the borders of three clusters of TADs
70 showing the lack of correlation with the inequality in directionality for three
71 clusters of TADs in *Drosophila* S2 cells. Data in **a** and **c** are represented as
72 mean±SEM.

73

74 **Supplementary Fig. 9|RNA expression was reduced after *rpb1***
75 **knock-down and transcription inhibition.**

76 **a**, RNA expression compared to s9 and s13 wild-type embryos after *rpb1* was
77 knocked-down.

78 **b**, RNA expression compared to s9 and s11 wild type embryos after
79 transcription inhibition.

80 RPKM, reads per kilobase of transcript, per million mapped reads.

81

82 **Supplementary Fig. 10 | Effects of *rpb1* knock-down on RPB2 binding.**

83 **a**, RPB2 expression in wild-type embryos at stages 8, 9, 11 and 13.

84 **b**, Western blot of proteins in embryos with RPB1 knocked-down by
85 morpholinos and in embryos that were rescued. Morpholino control (ctrl), no
86 morpholino (-), *rpb1* morpholino (+), *rpb1* rescue (rsc). Western blot
87 experiments in this figure were repeated for at least two times with similar
88 results.

89 **c**, RPB2 ChIP-seq signal across genes normalized to spike-in K562.
90 **d**, RPB2 ChIP-seq signal across human genes in spike-in K562 cells. For **c** &
91 **d**, Wild type (wt), morpholino control (ctrl), *rpb1* morpholino knock-down (*rpb1*
92 kd), *rpb1* rescue (*rpb1* rsc), all experiments were conducted in two biological
93 replicates.

94

95 **Supplementary Fig. 11|CTCF ChIP-seq for knock-down analysis.**

96 **a**, CTCF ChIP-seq for CTCF and Rad21 knock-down experiments normalized
97 to spike-in K562.

98 **b**, CTCF ChIP-seq for K562 cells spiked-in CTCF and Rad21 knock-down
99 experiments. Wild type (wt), morpholino control (ctrl), *ctcf* morpholino (*ctct* kd),
100 *ctcf* rescue (*ctcf* rsc), *rad21* morpholino (*rad* kd), *rad21* rescue (*rad* rsc), *ctcf*
101 and *rad21* morpholinos (*dbl* kd), *ctcf* and *rad21* rescue (*dbl* rsc), all
102 experiments were carried out in two biological replicates.

103

104 **Supplementary Fig. 12|Rad21 ChIP-seq for knock-down analysis.**

105 **a**, Rad21-ChIP seq for CTCF and Rad21 knock-down experiments normalized
106 to spike-in K562.

107 **b**, Rad21-ChIP seq for K562 cells spiked-in CTCF and Rad21 knock-down
108 experiments. Wild type (wt), morpholino control (ctrl), *ctcf* morpholino (*ctct* kd),
109 *ctcf* rescue (*ctcf* rsc), *rad21* morpholino (*rad* kd), *rad21* rescue (*rad* rsc), *ctcf*
110 and *rad21* morpholinos (*dbl* kd), *ctcf* and *rad21* rescue (*dbl* rsc), all

111 experiments were carried out in two biological replicates.

112

113 **Supplementary Fig. 13|Effects of *ctcf* and *rad21* knock-down on**
114 **chromatin structure.**

115 **a**, Example region to show the knock-down effect on TAD structures.

116 **b**, Correlation of insulation scores for the borders of identified TADs in wild
117 type embryos at s13 vs control, knock-down, and rescued embryos at s13.

118 **c**, Number of TADs and size distribution.

119 **d**, Percentage of genome folds into TADs.

120

121 **Supplementary Fig. 14 | Effects of *ctcf* and *rad21* knock-down on embryo**
122 **development.** Knock-down of *ctcf* and *rad21* were repeated for at least two
123 times with similar results.

124

125 **Supplementary Fig. 15|CTCF ChIP-seq on *snf2h* knock-down cells.**

126 **a**, CTCF ChIP-seq on *snf2h* knock-down embryos normalized to spike-in K562
127 signal.

128 **b**, CTCF ChIP-seq on spike-in K562 cells. Wild type (wt), morpholino control
129 (ctrl), *snf2h* morpholino (*snf2h* kd), *snf2h* rescue (*snf2h* rsc), all experiments
130 were conducted in two biological replicates.

131

132 **Supplementary Fig. 16 | Effects of *snf2h* knock-down.**

133 **a**, Number of TADs and TAD size distribution.
134 **b**, Percentage of genome folds into TADs.
135 **c**, Effect of *snf2h* knock-down on embryo development. Knock-down of *snf2h*
136 were repeated for at least two times with similar results.

137

138 **Supplementary Fig. 17|Chromatin contact heatmaps.**

139 Heatmaps of 50kb resolution for a 30Mb region in chromosome 2 from multiple
140 developmental stages show continuous compartmentalization.

141

142 **Supplementary Fig. 18|Coincident localization of TAD border with**
143 **hierarchical TAD border and compartment switch regions in stage 13**
144 **embryos of *X. tropicalis*.**

145 **a**, Percentage of the three clusters TAD that overlap with hierarchical TAD or
146 being singleton TAD.

147 **b**, Number of TADs from cluster 1 and cluster 3 that are paired in hierarchical
148 TAD.

149 **c**, Percentage of the three clusters TAD that overlap with compartment switch
150 region with random genomic regions as background control.

151

152 **Supplementary Fig. 19|. Diamond areas for domain “diamond score”**
153 **calculation.** M, U, and D denote the middle, upstream, and downstream
154 diamond areas of the domain (black triangle).

155

156 **Supplementary Table 1 | Comparison of the three versions of the *Xenopus***
157 ***tropicalis* reference genome.**

158

159 **Supplementary Table 2 | PacBio sequencing statistics.**

160

161 **Supplementary Table 3 | Hi-C sequencing statistics.**

162

163 **Supplementary Table 4 | Gene sequences for rescue experiments.**

164

165 **Supplementary Table 5 | Morpholino antisense oligonucleotides for**
166 **knock-down experiments.**

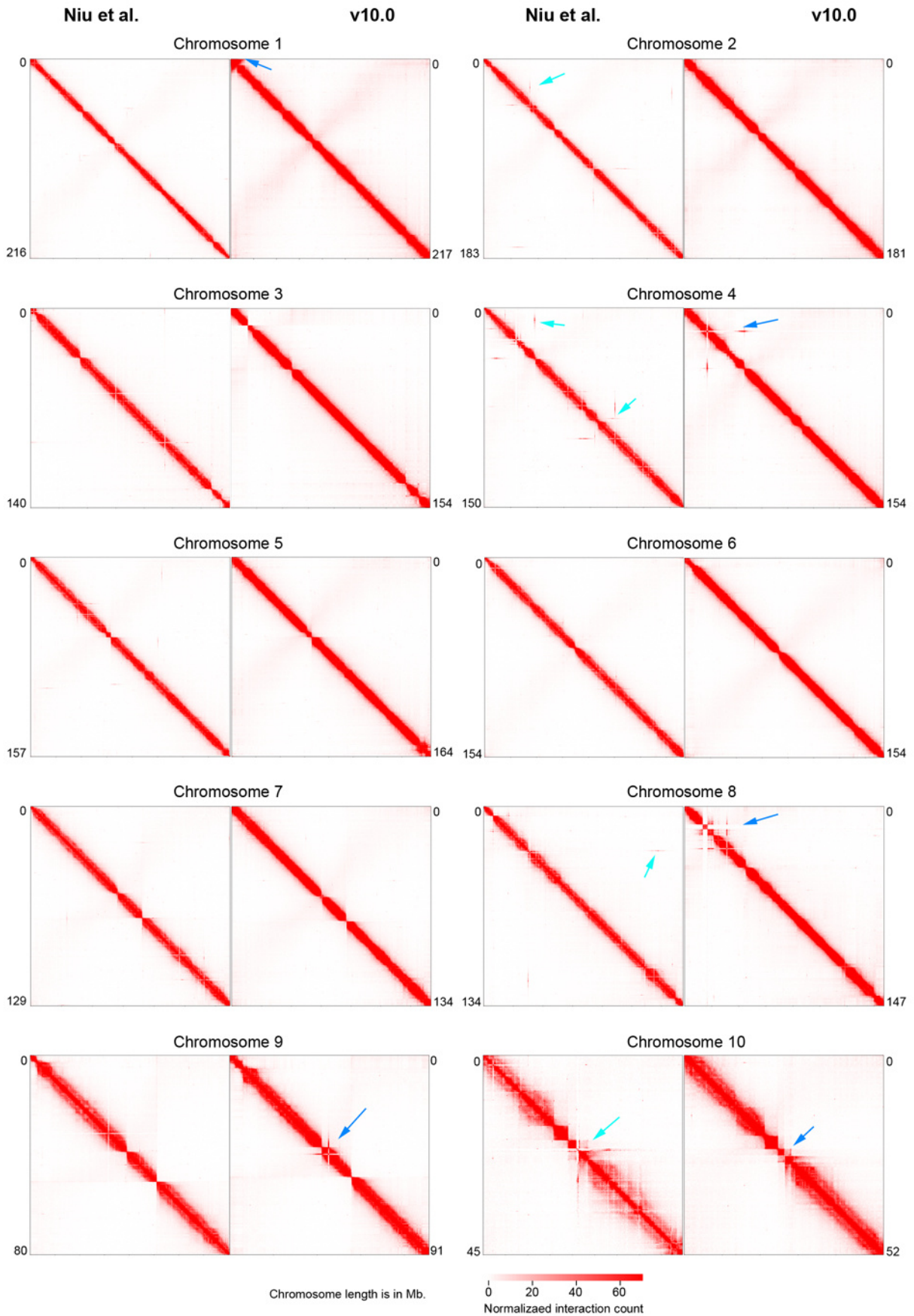
167

168 **Niu_SourceData_SupplementaryFig3b**

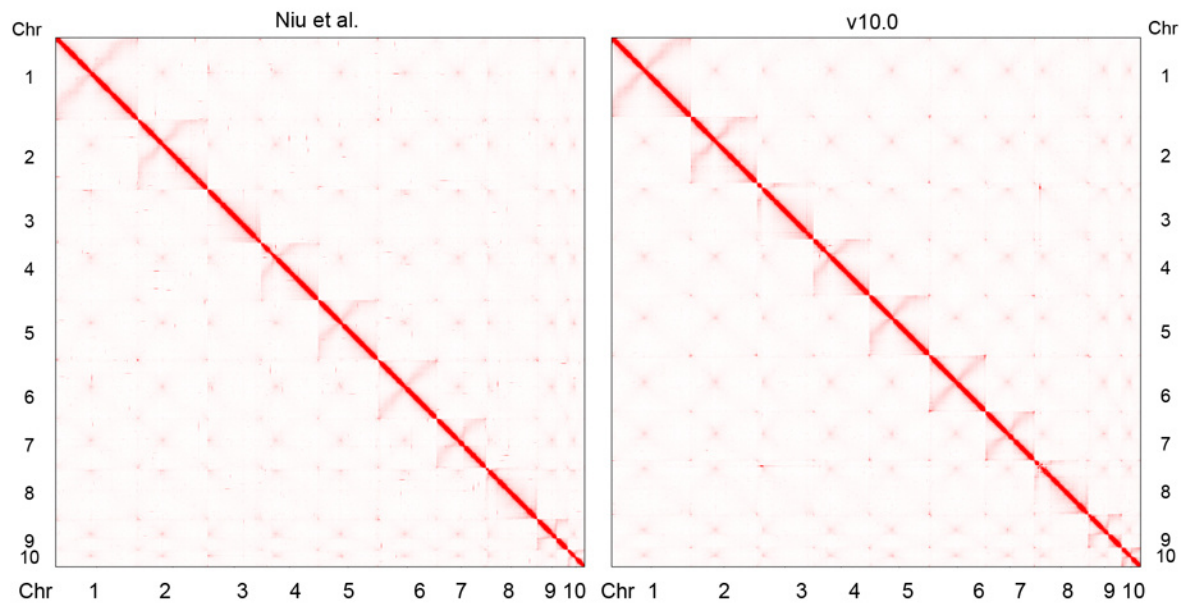
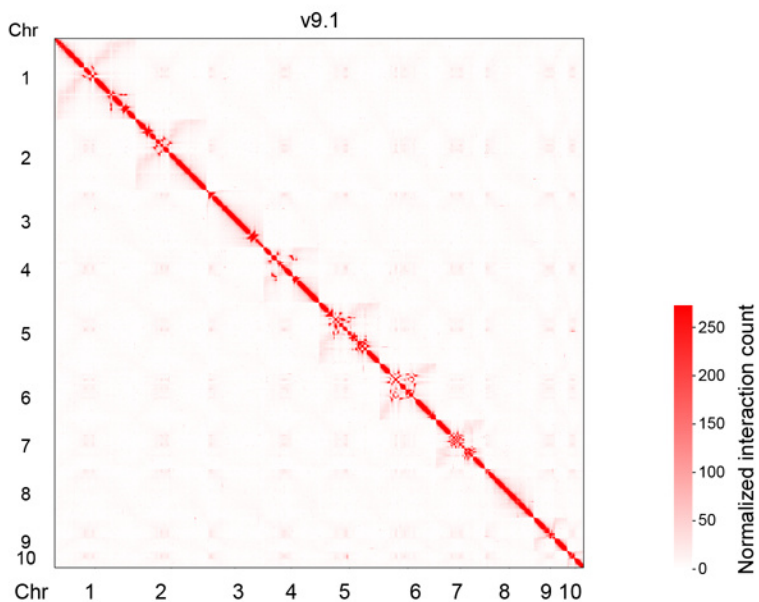
169 **Niu_SourceData_SupplementaryFig10a**

170 **Niu_SourceData_SupplementaryFig10b**

Supplementary Fig. 1

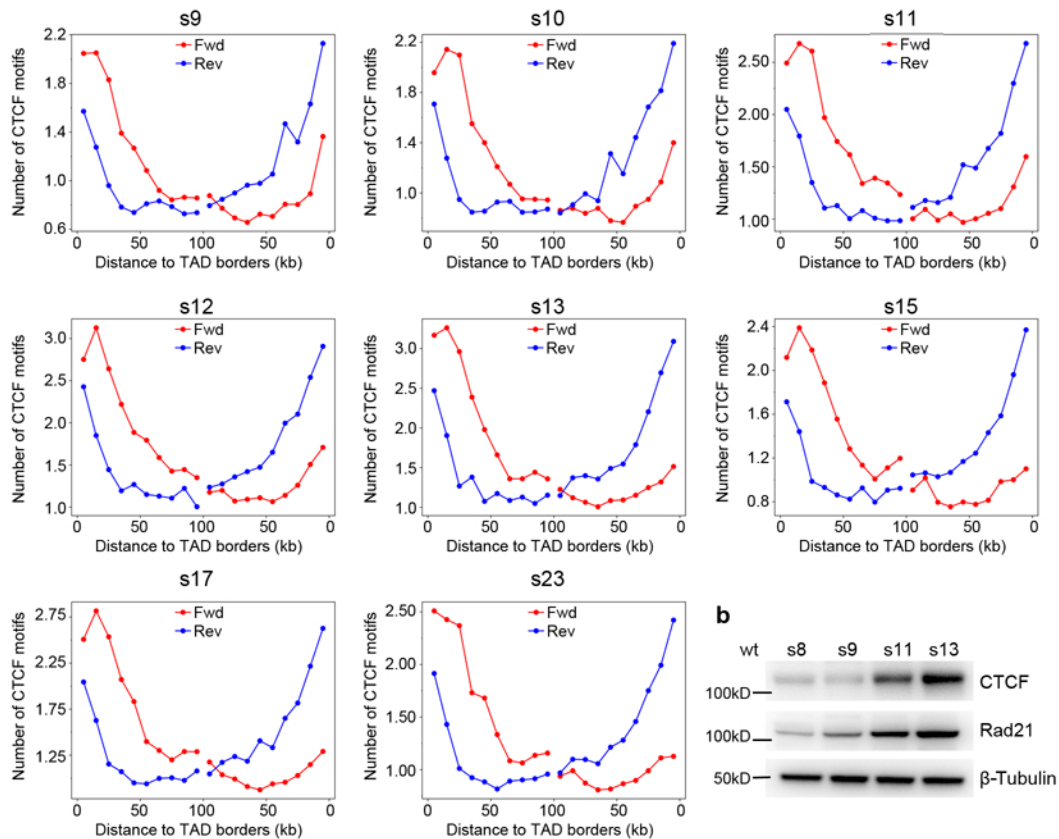


Supplementary Fig. 2



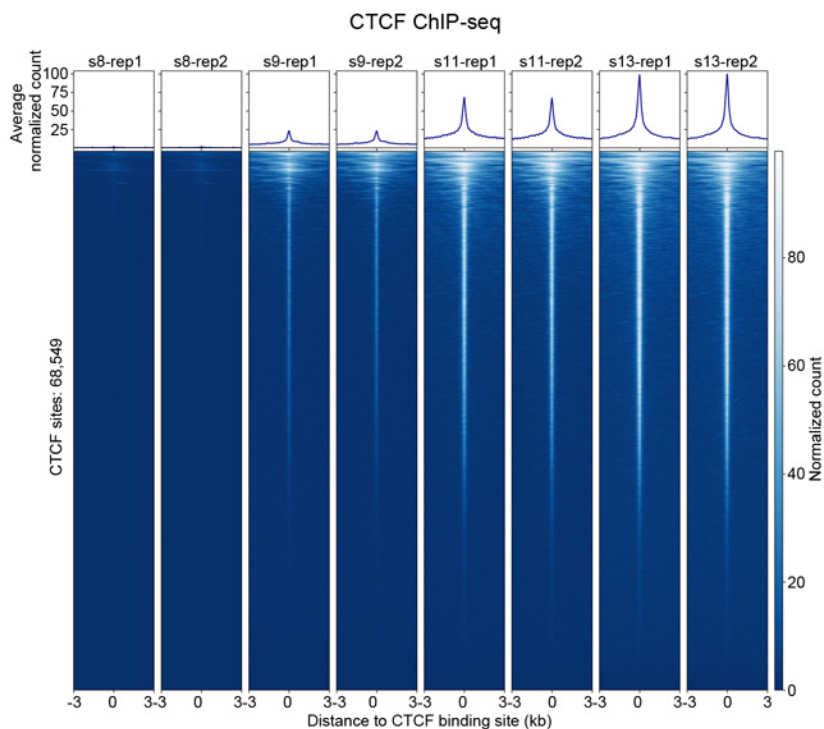
Supplementary Fig. 3

a



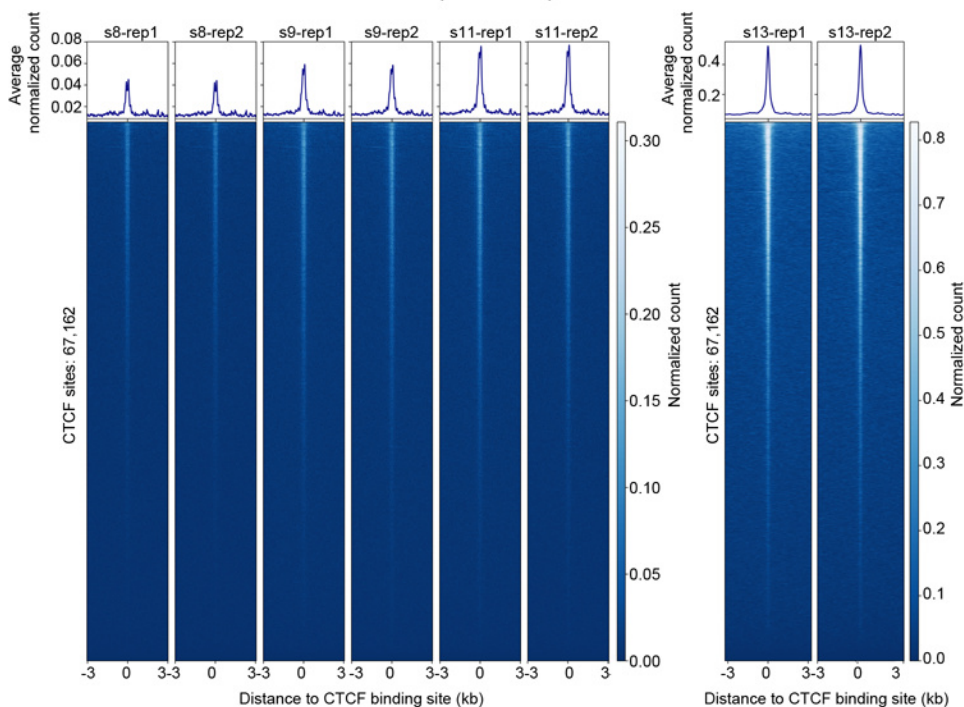
Supplementary Fig. 4

a



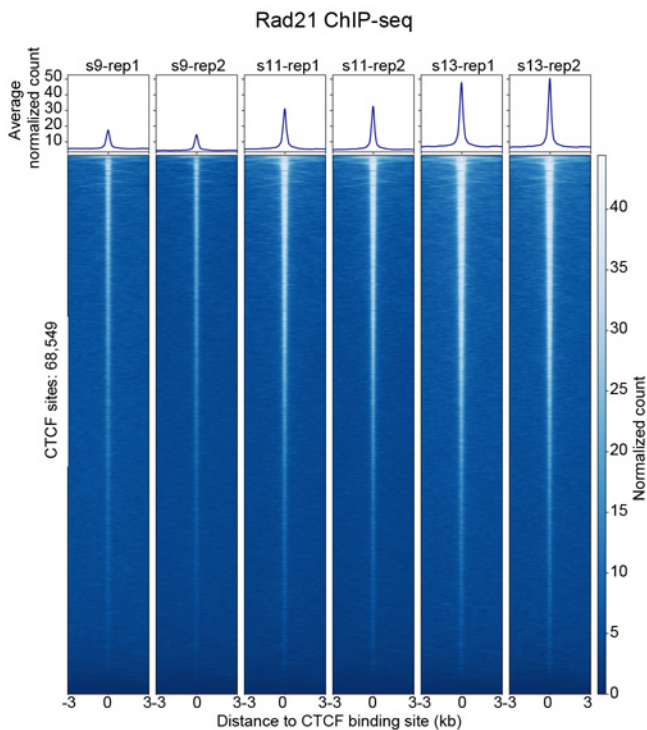
b

CTCF ChIP-seq for K562 spike-in cells

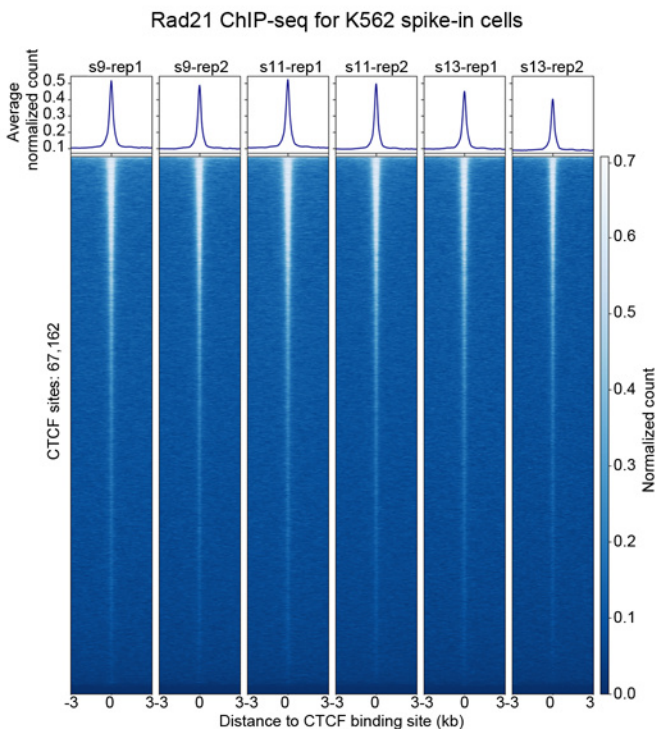


Supplementary Fig. 5

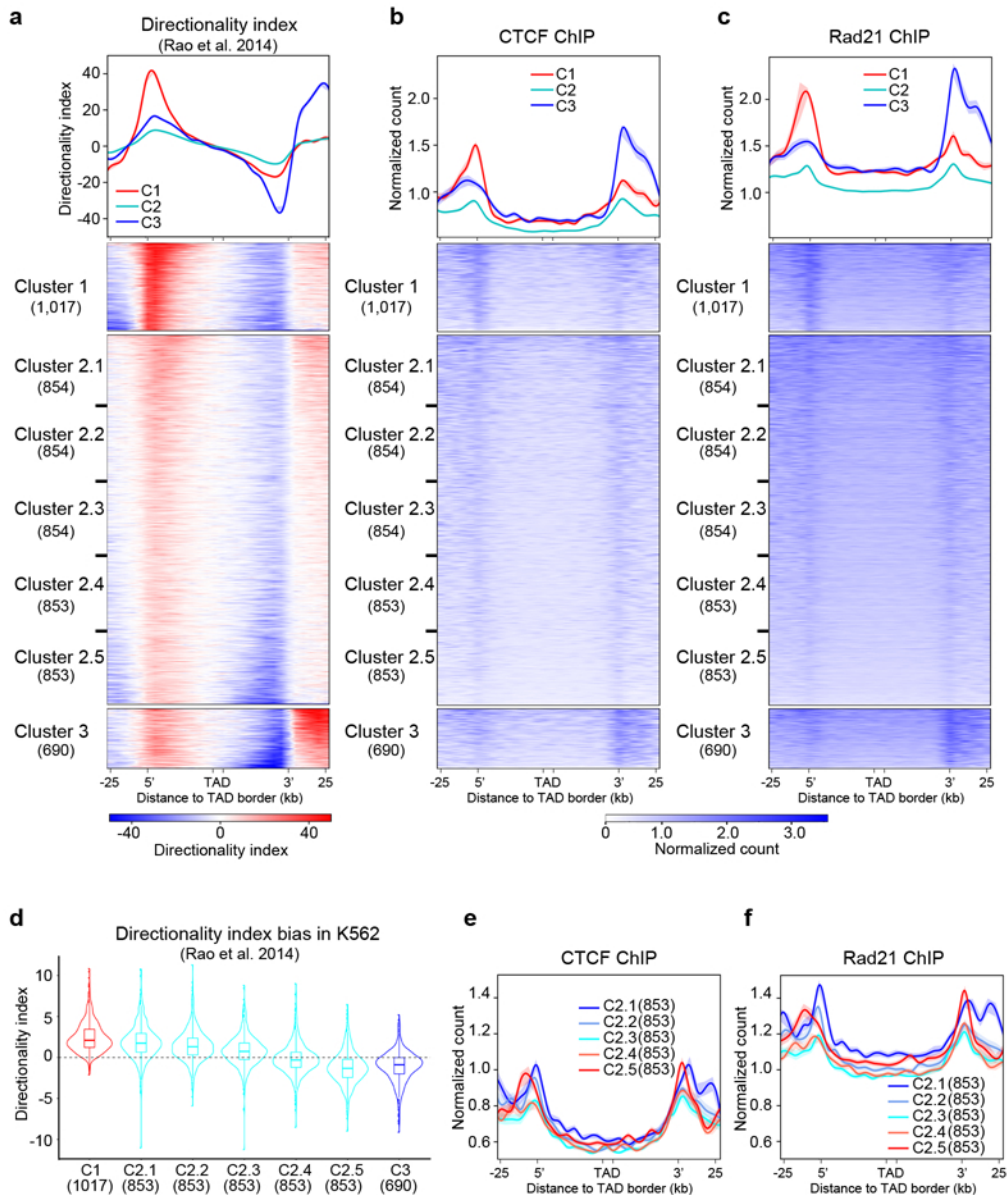
a



b

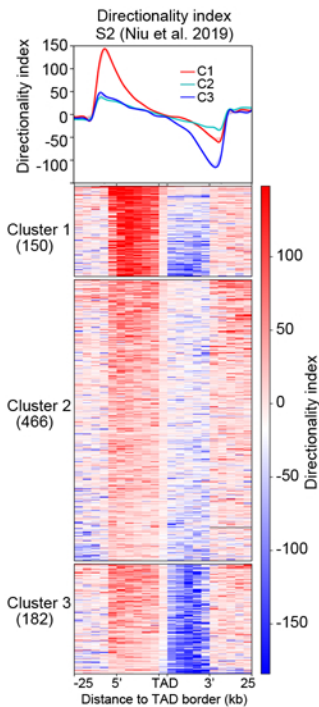


Supplementary Fig. 7

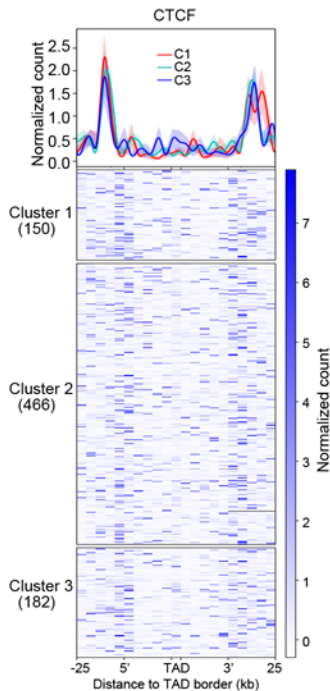


Supplementary Fig. 8

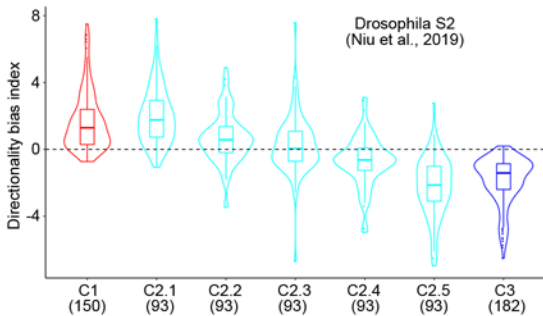
a



c

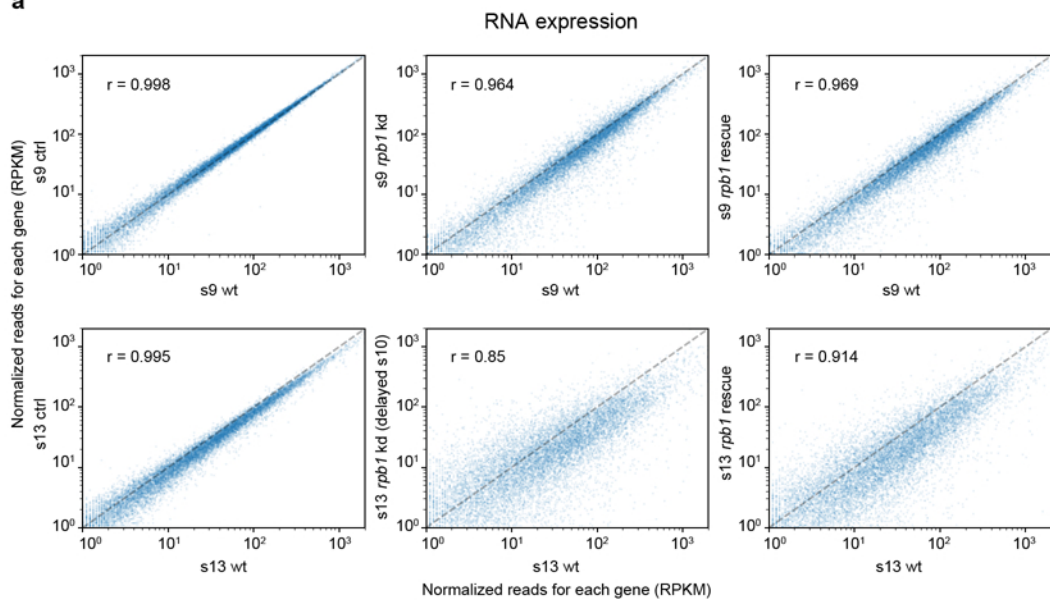


b

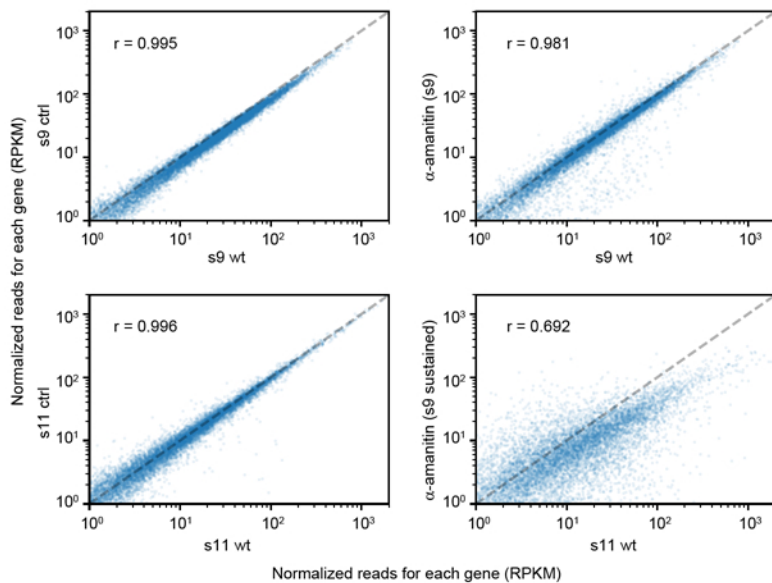


Supplementary Fig. 9

a

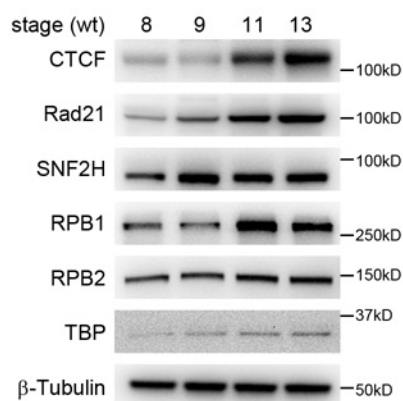


b

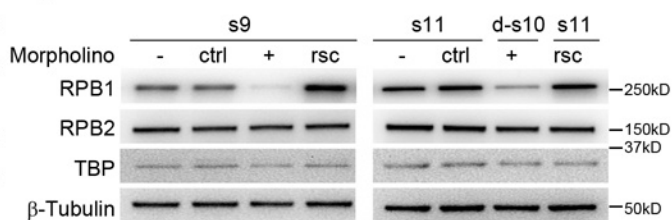


Supplementary Fig. 10

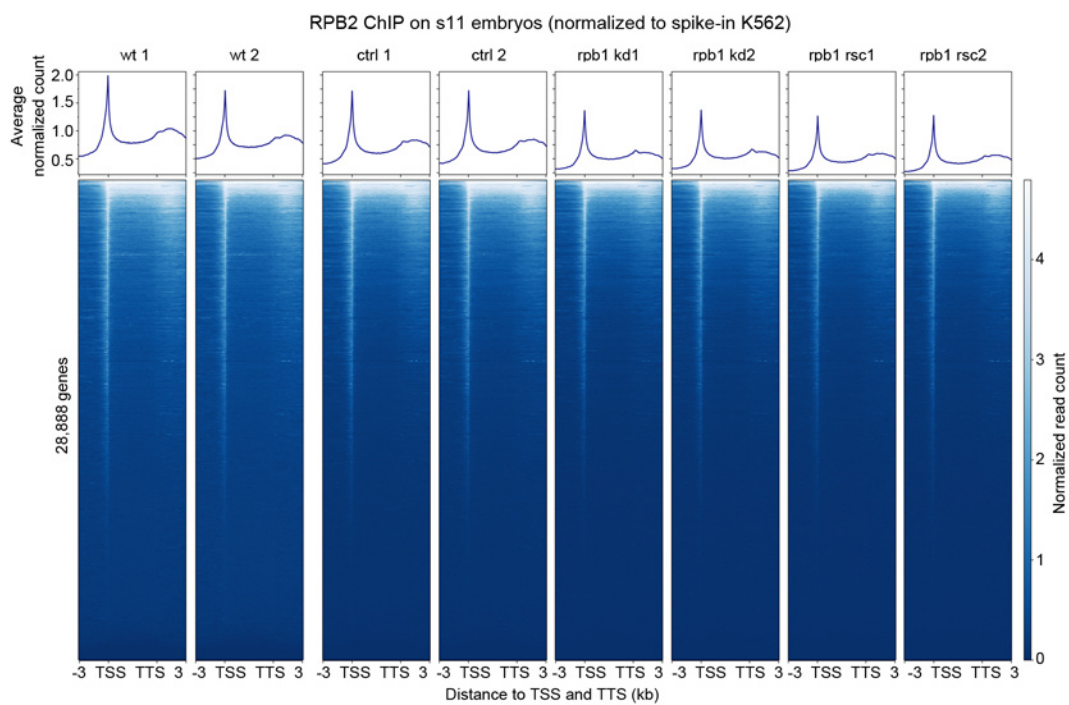
a



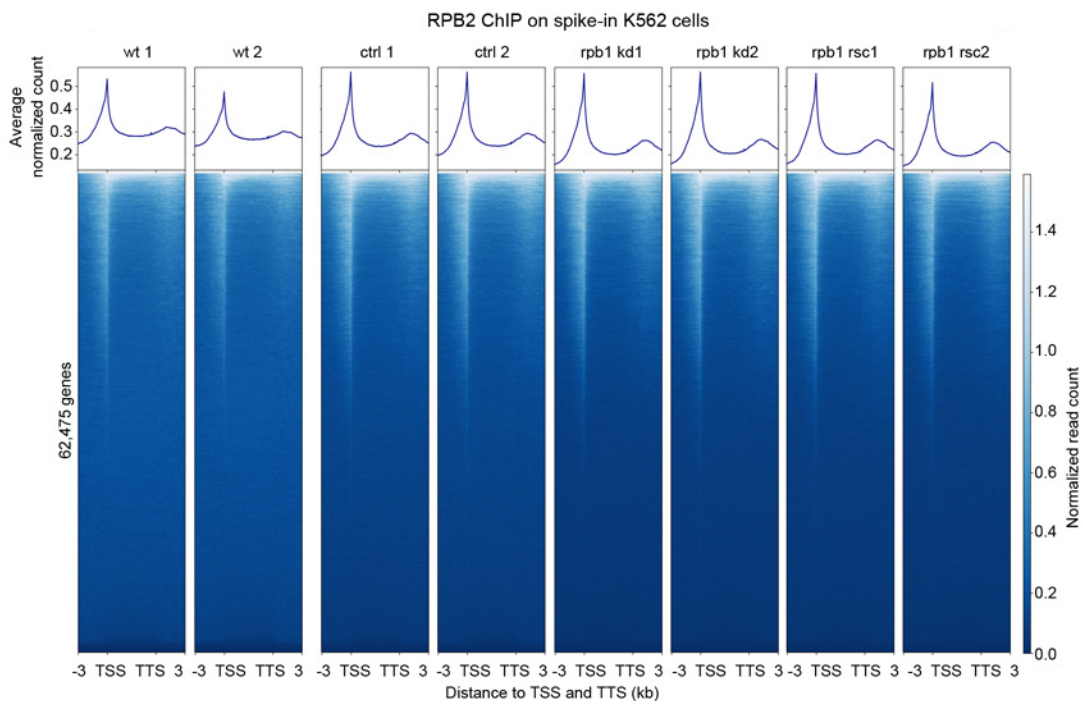
b



c

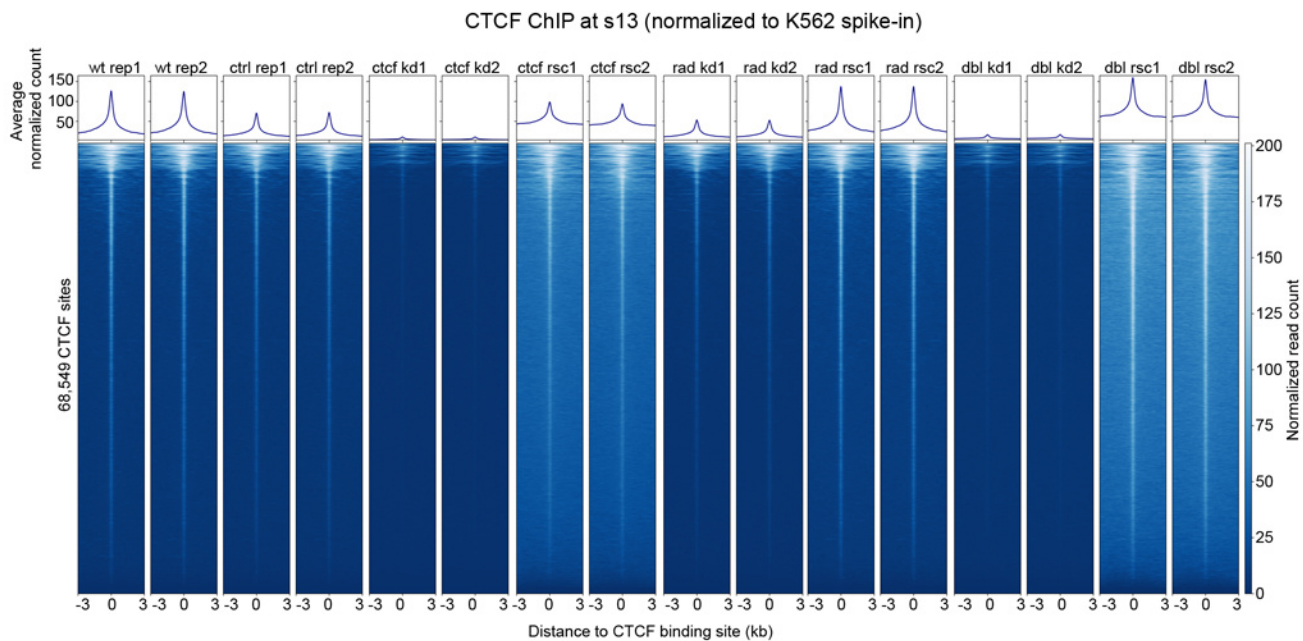


d

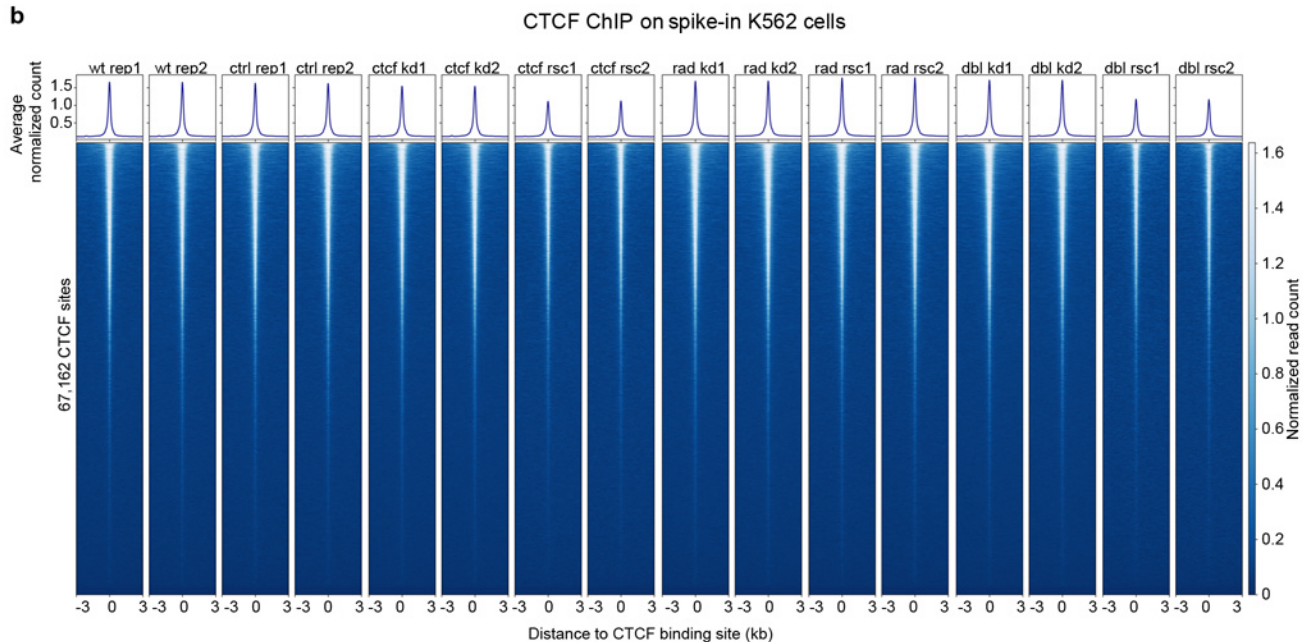


Supplementary Fig. 11

a



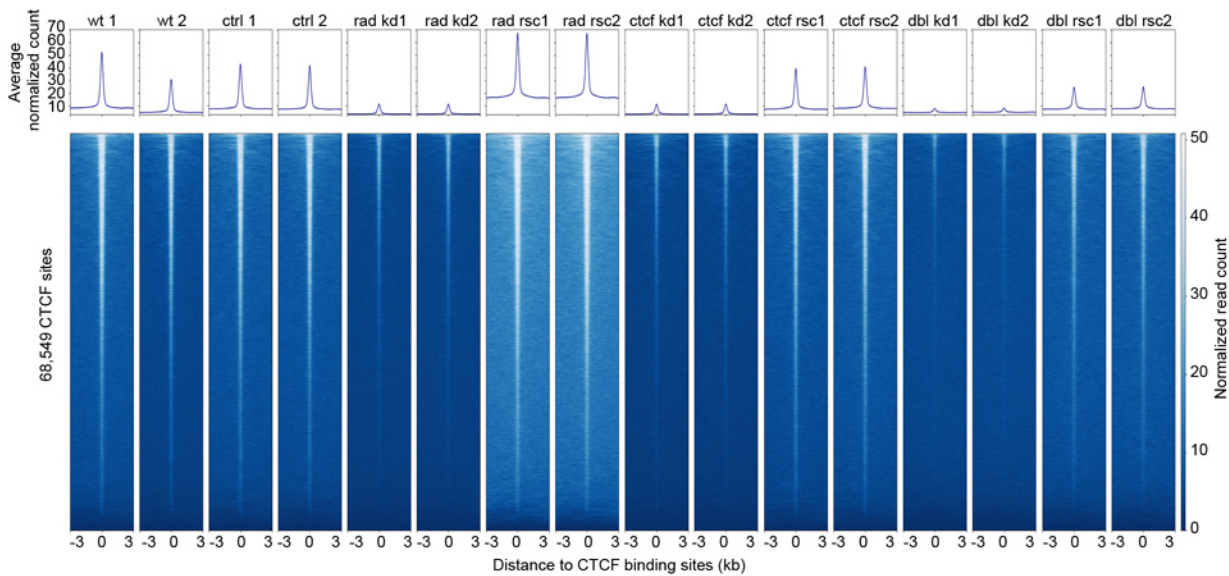
b



Supplementary Fig. 12

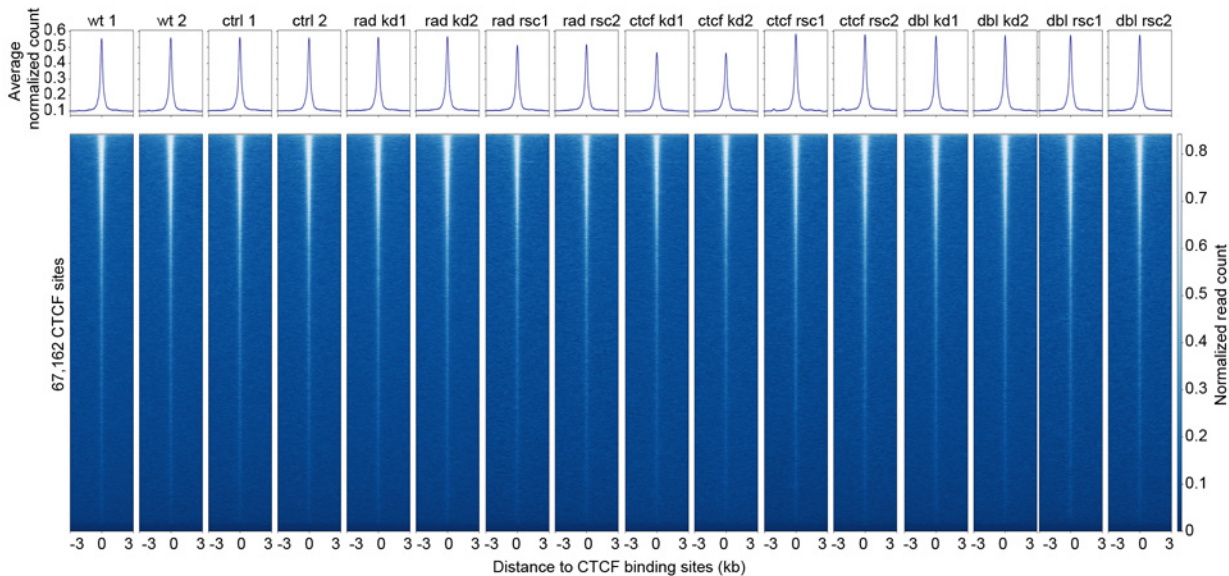
a

Rad21 ChIP-seq at s13 (normalized to K562 spike-in)

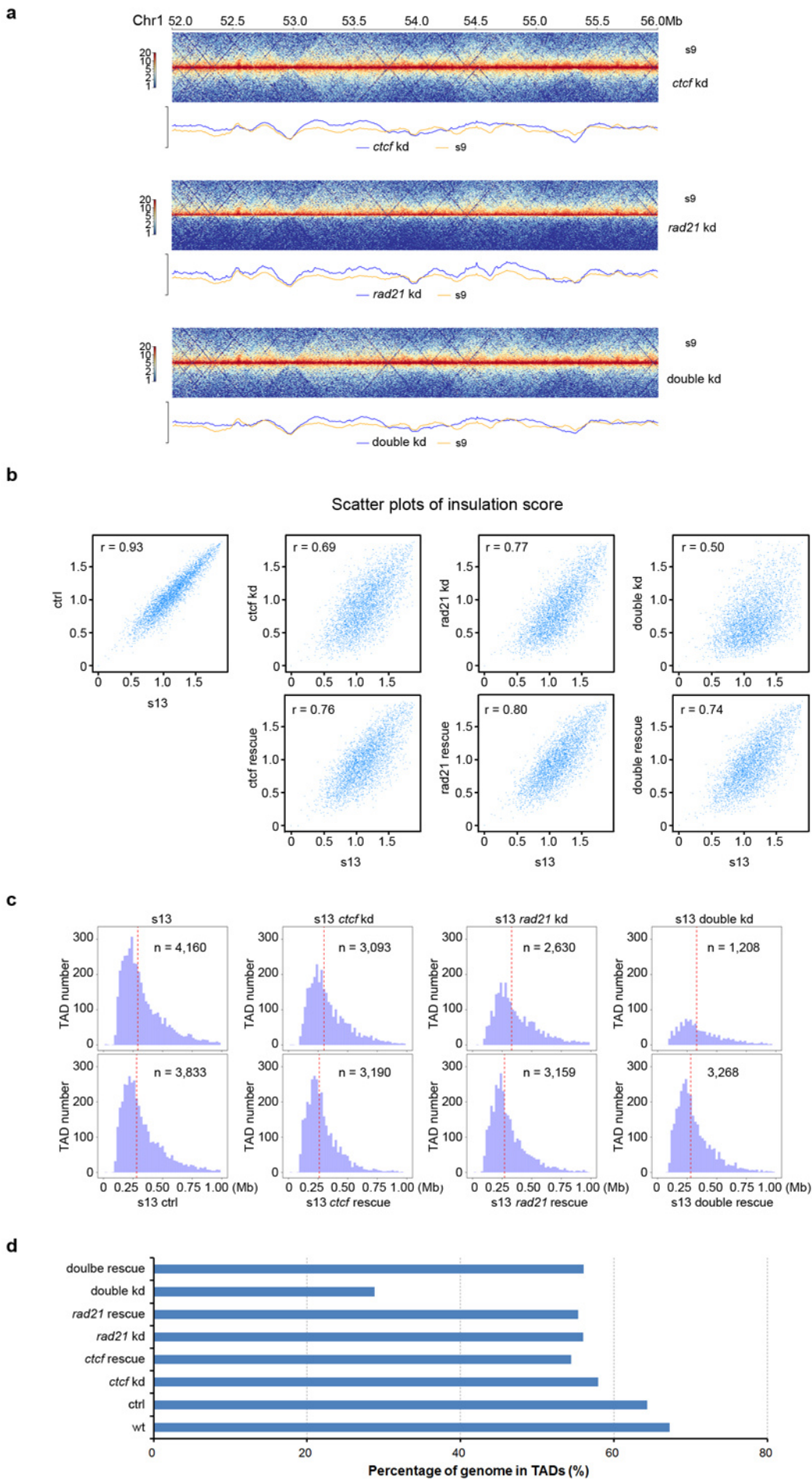


b

Rad21 ChIP-seq on spike-in K562 cells

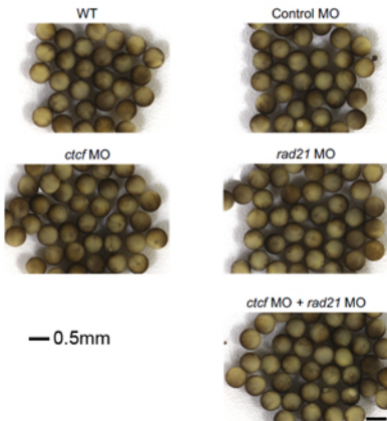


Supplementary Fig. 13



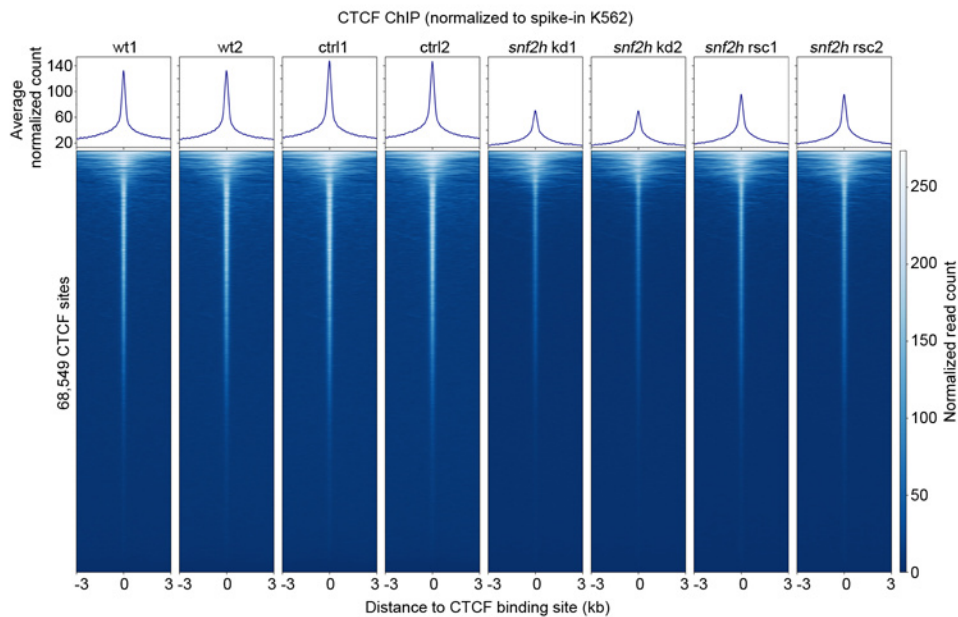
Supplementary Fig. 14

All embryos were at s13.

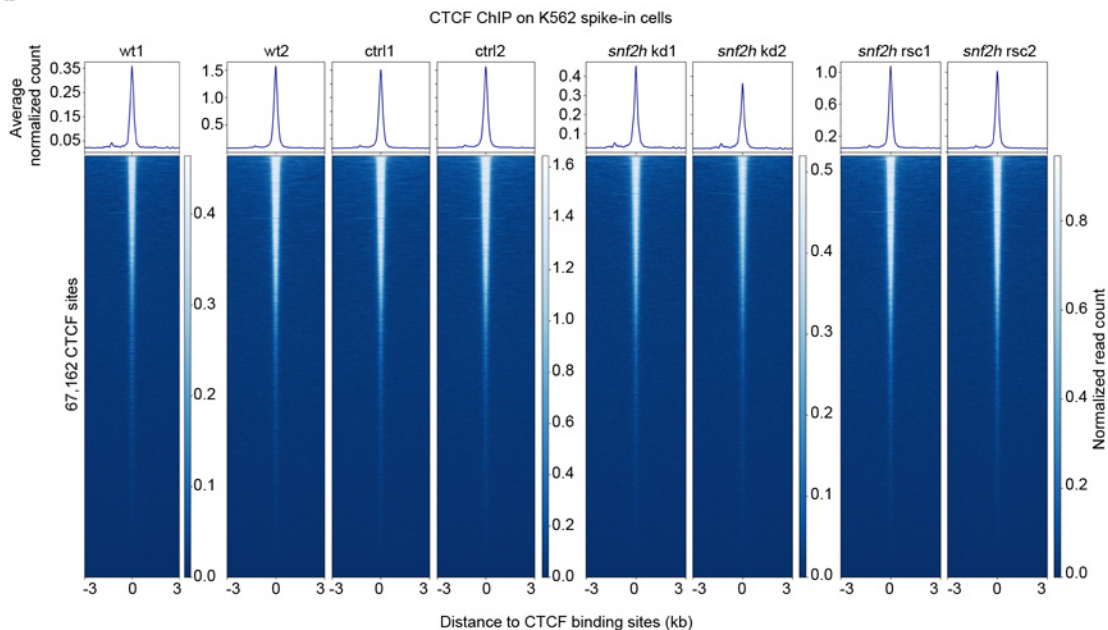


Supplementary Fig. 15

a

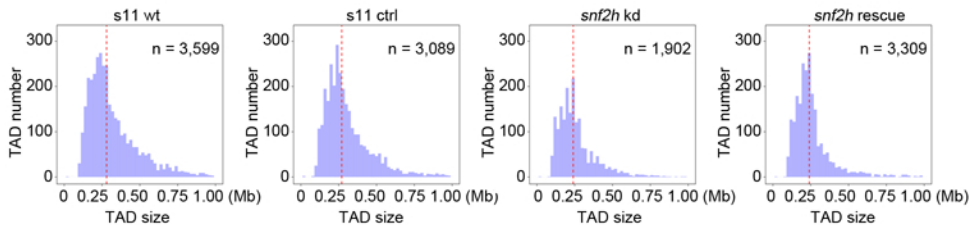


b

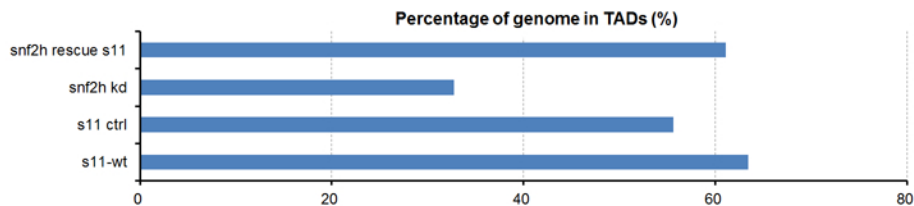


Supplementary Fig. 16

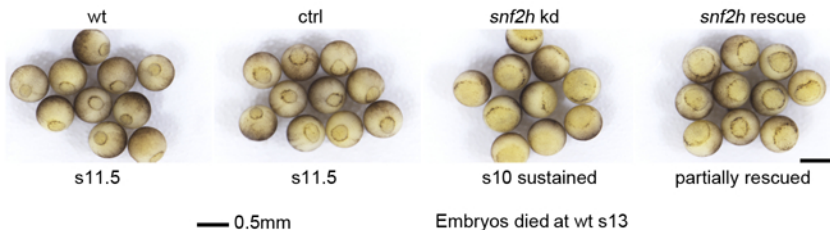
a



b

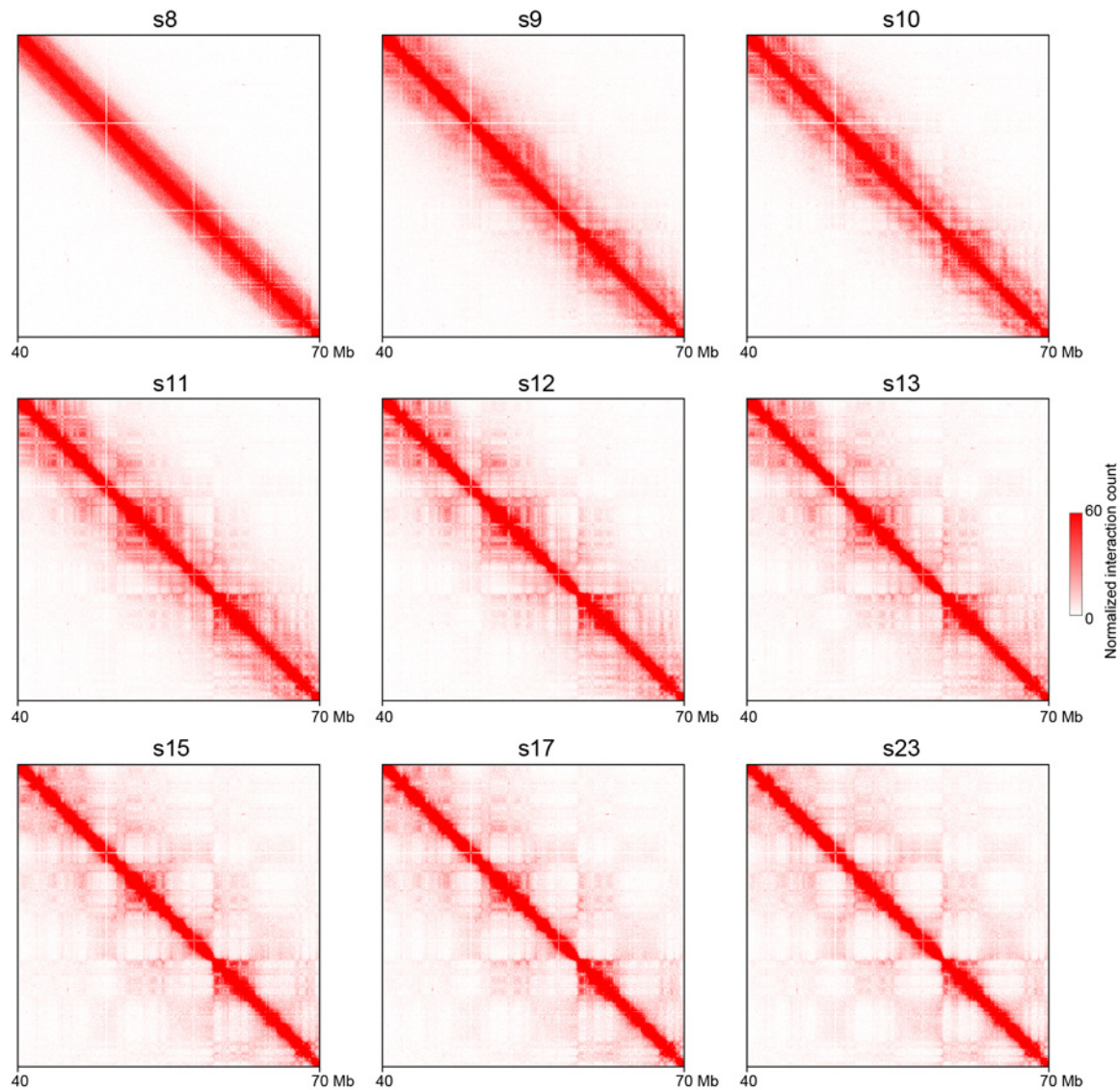


c



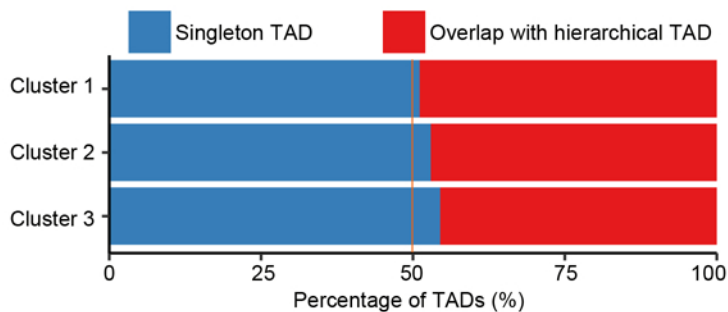
Supplementary Fig. 17

Chromosome 2

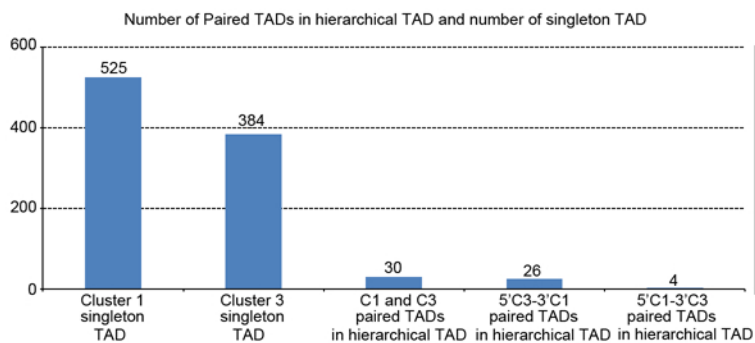


Supplementary Fig. 18

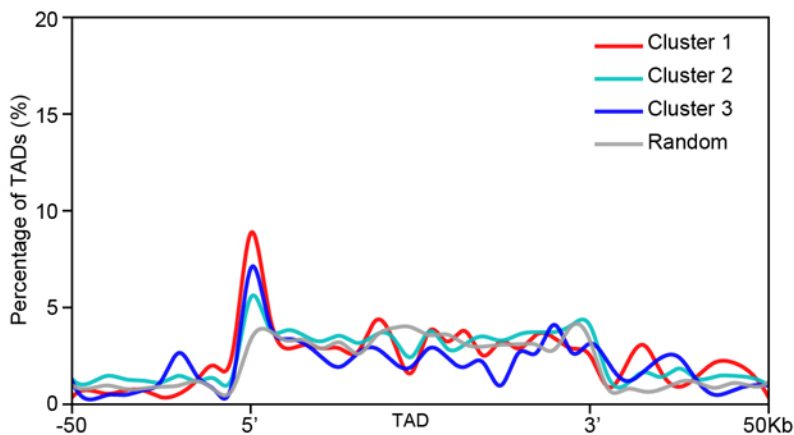
a



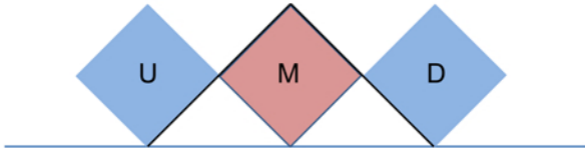
b



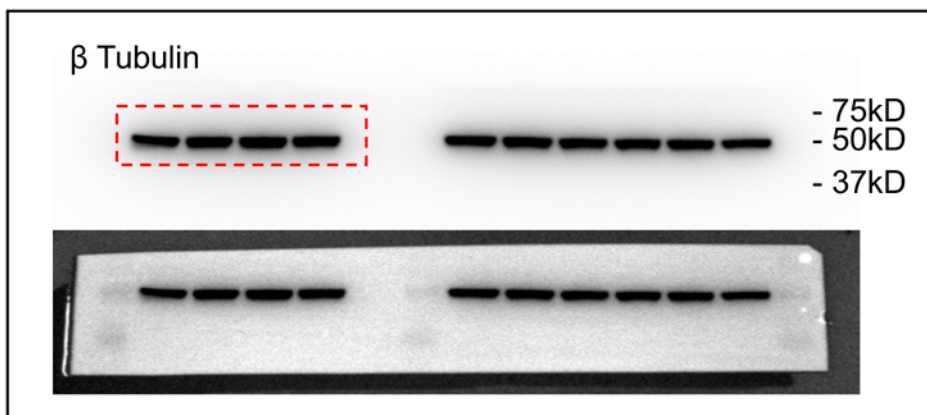
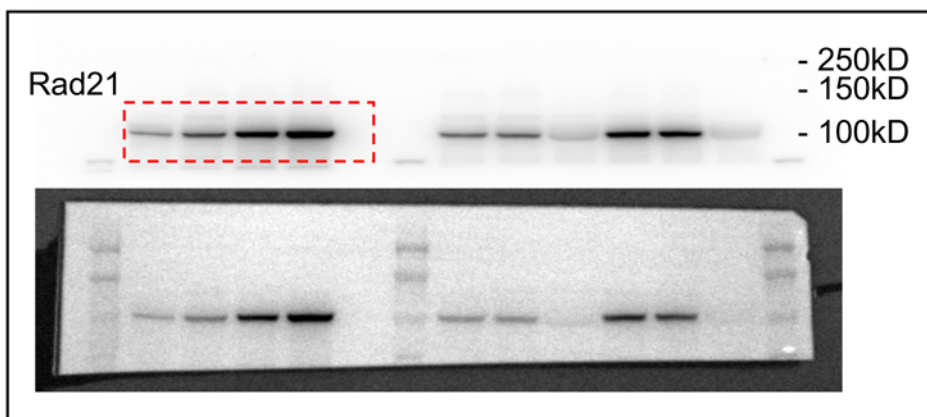
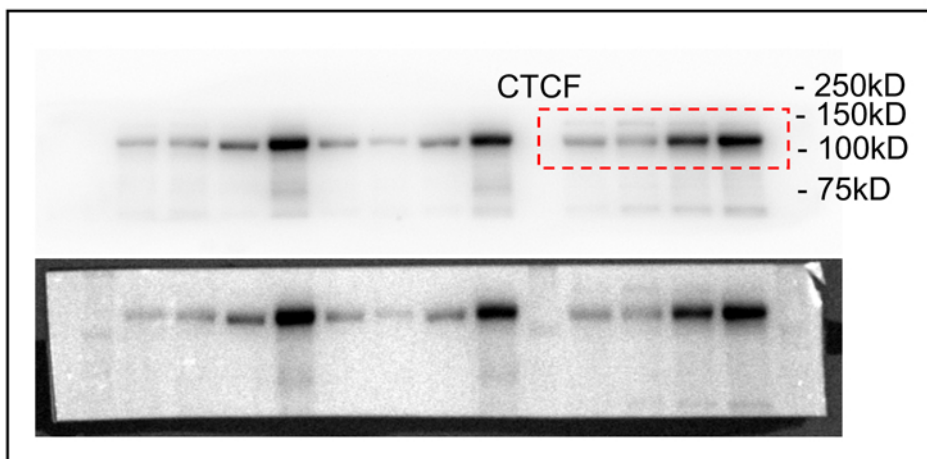
c



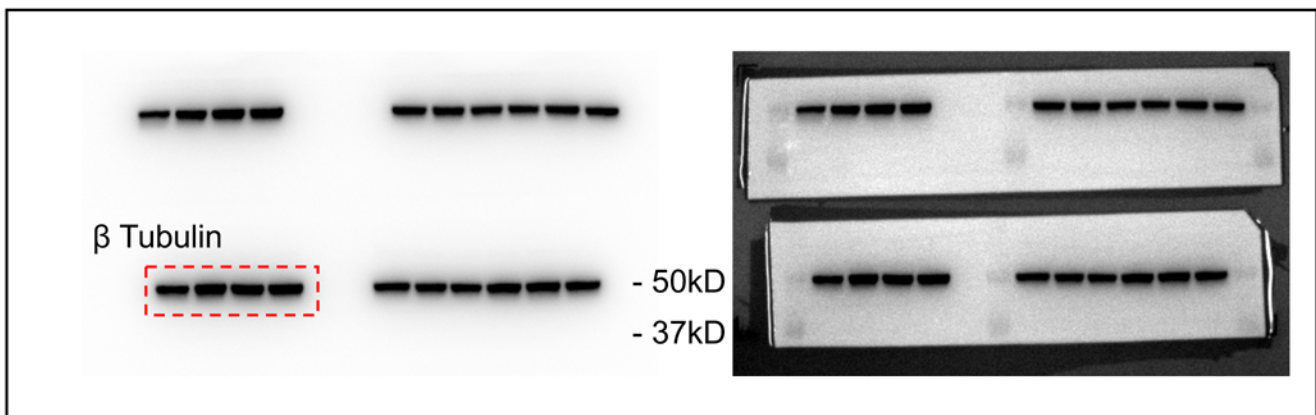
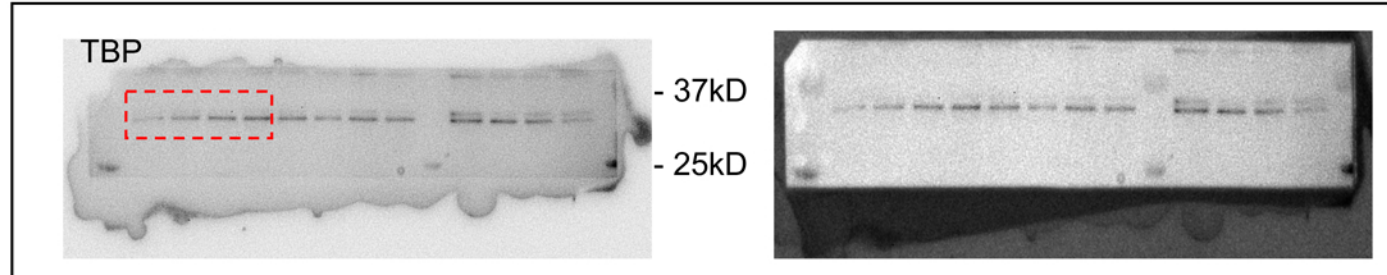
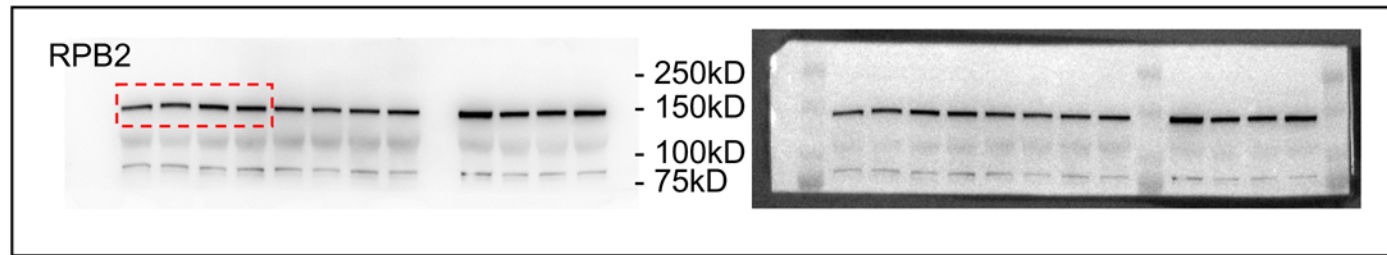
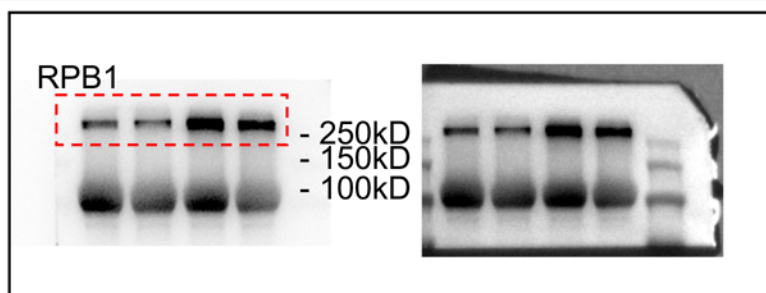
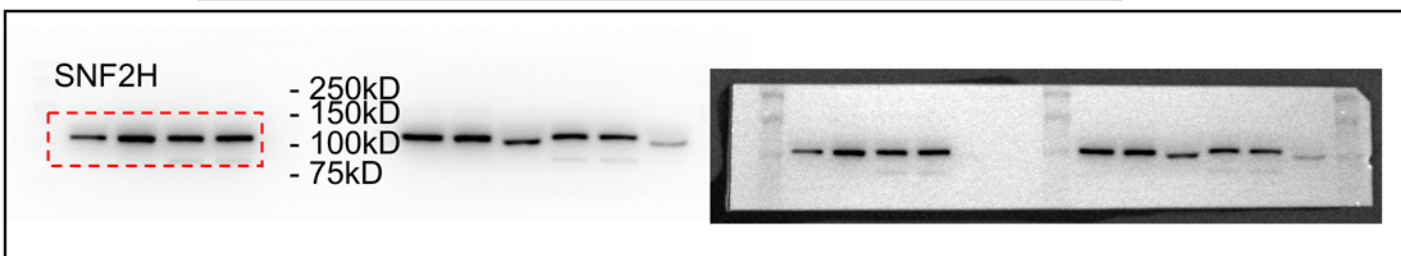
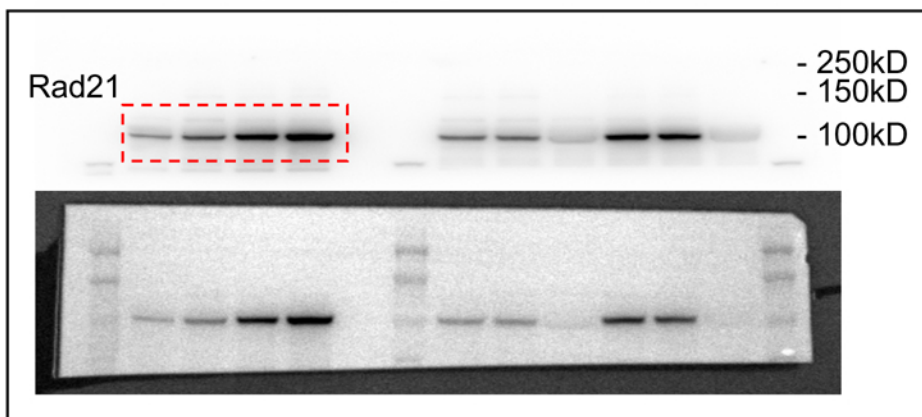
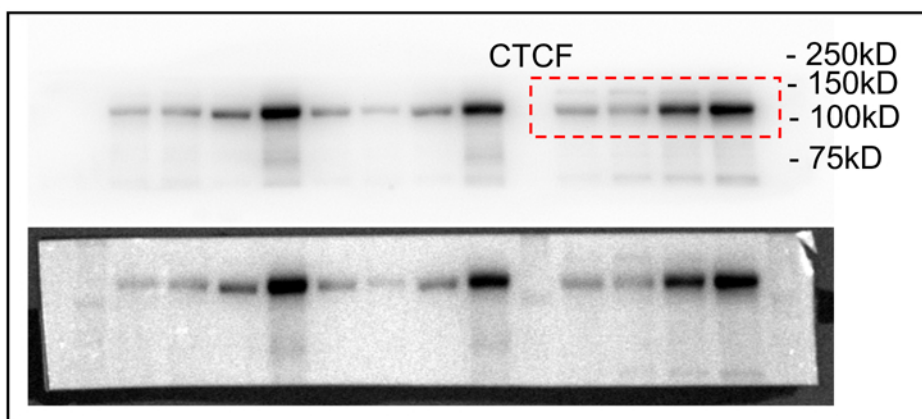
Supplementary Fig. 19



SourceData for Supplementary Fig. 3b

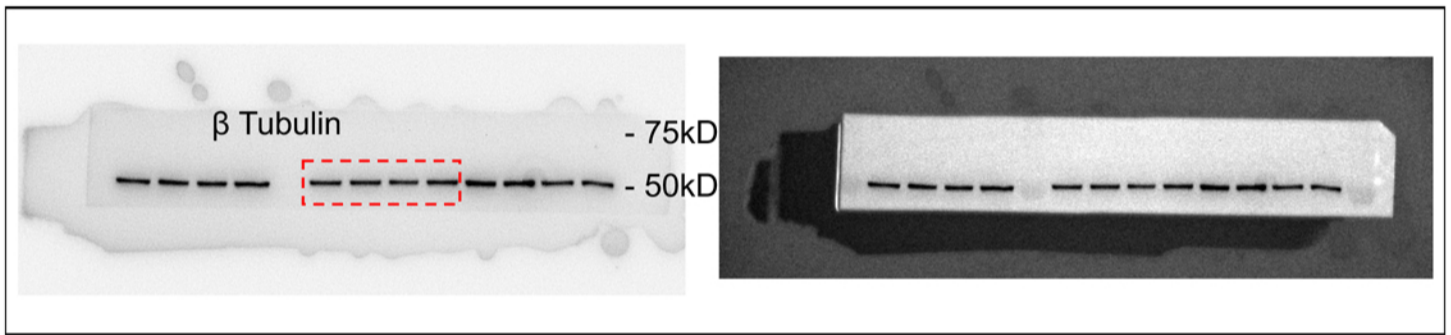
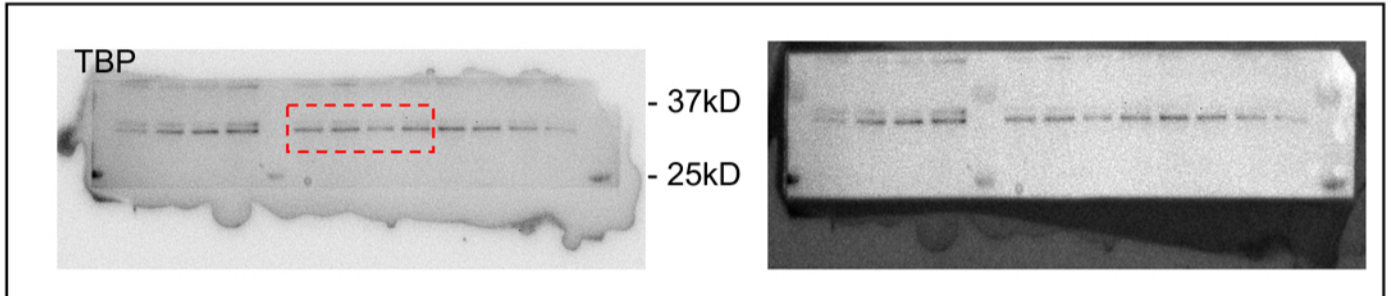
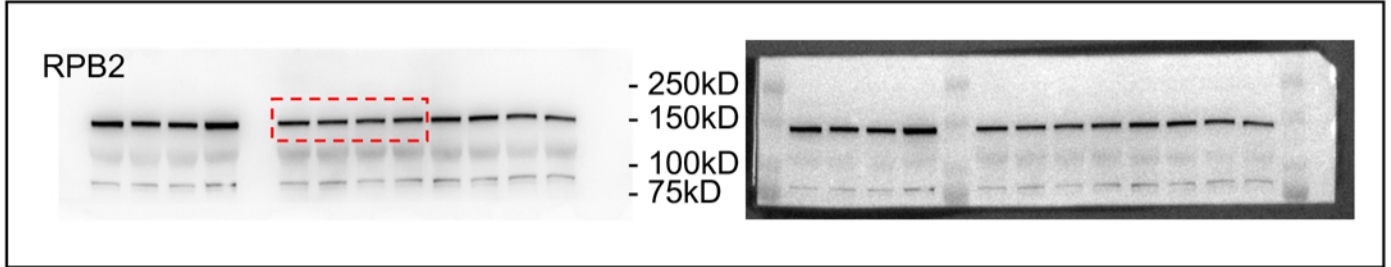
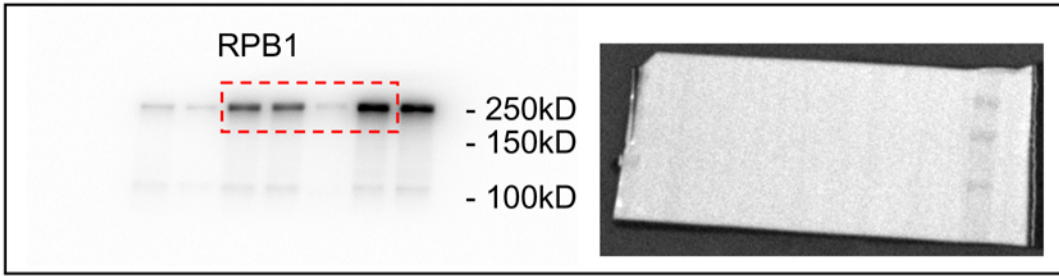


Supplementary Fig. 10a



Supplementary Fig. 10b

st 9



st 11

